ARTICLE NO. 79-0258R

A80-035

Aerodynamic Characteristics for Debris from Space Shuttle External Tank

40002

S.P. Bonson*
Martin Marietta Corporation, New Orleans, La.

This paper develops a methodology to determine effective values of the aerodynamic parameters required for performing simplified three-degree-of-freedom debris impact analyses rather than utilizing more complex six-degree-of-freedom analyses. For all of the debris types, six-degree-of-freedom mass property and aerodynamic data are computed. Using the results of many six-degree-of-freedom trajectory simulations, standard deviation range values are calculated. With three-degree-of-freedom trajectory matching, these range values are used to determine the effective ballistic coefficient and the range of lift-to-drag ratios for each of the External Tank debris types defined.

Introduction

THE External Tank is jettisoned from the Space Shuttle Orbiter just before reaching orbital velocity. During entry, it breaks up into various pieces of debris which are spaced over a long, very narrow footprint. To predict the size of this footprint, it is necessary to have the aerodynamic characteristics and their statistical variations for each piece of debris.

The theory and methodology are presented for analytically determining the aerodynamic parameters required for a three-degree-of-freedom (3-DOF) calculation of the entering External Tank (ET) debris footprint. Mass property and aerodynamic characteristics were generated consistent with 6-DOF trajectory simulation. Standard deviation (1-σ) range values were derived from the 6-DOF trajectory simulation. These range values were used to determine the effective aerodynamic parameters: the ballistic coefficient W/C_DA with its corresponding 1-σ lift-to-drag ratio, L/D. The term "effective" is used for the aerodynamic characteristics data since they are derived from the range dispersions of the 6-DOF trajectory simulations. The "3-σ" L/D ratio values are derived from the 3-σ 6-DOF range values.

The need for this study was indicated when it was realized that there were no analyses verifying the aerodynamic characteristics being used in simulating entry of debris. Prior to development of the present technique, W/C_DA values were based on average tumbling drag coefficients, while L/D ratio dispersions were based on assumed values, 0.2 having been defined for the ET disposal footprint analyses.

Figure 1 represents an "exploded" view of the ET. The skin-structure temperature data at ET disintegration were used to determine the potential debris types.[1] The classes of debris predicted and analyzed include: 1) medium to large sized skin panels; 2) pipe, tubing, and conduit; 3) ring frames; 4) the intertank structure, including domes from both the oxygen (LO_2) and hydrogen (LH_2) tanks; and 5) the aft support-structure including the ET/Orbiter and ET/Solid Rocket Booster (SRB) attachment hardware.

The purpose of this study was to establish analytically a method of using 6-DOF trajectory simulations to determine the W/C_DA and associated 3-σ L/D ratio dispersions for the several debris types that exist at ET disintegration.

Presented as Paper 79-0258 at the 17th Aerospace Sciences Meeting, New Orleans, La., Jan. 15-17, 1979; submitted Jan. 29, 1979; revision received Oct. 3, 1979.

Index category: LV/M Aerodynamics.

*Design Engineer, Systems Performance Dept.

Assumptions

The following assumptions are required for the aerodynamic characteristics analysis described herein:

1) The defined debris types exist at ET breakup. This assumption is confirmed by detailed studies.[1] The actual shape of debris types can be represented by the shapes assumed for this study.

2) Hypersonic aerodynamic coefficients are analytically derived for the selected debris types. These hypersonic aerodynamic coefficients[2,3] are assumed valid during the entire trajectory. Supersonic and subsonic data are not required because less than 19 mi. of range is accumulated between Mach 4 and impact.

3) The 6-DOF debris impact range data (per individual debris type) are normally distributed about the mean.

4) The effective aerodynamic parameters generated for each debris type consist of a value of W/C_DA and a range of values of L/D (expressed as a mean value with positive and negative dispersions). The value of W/C_DA selected is the one which leads to equal positive and negative dispersions of L/D from the 6-DOF standard deviation impact range calculation.

5) Small weight changes between simulated and actual debris can be incorporated in the weight part of the W/C_DA. The L/D will be unchanged.

6) Changes in mass property and aerodynamic characteristic due to melting are ignored.

Methodology

Debris types were identified from the ET breakup analyses of Ref. 1. While the exact size and shape of some of the debris types could not be completely defined, generalized definitions were selected that allowed estimation of the 6-DOF hypersonic aerodynamic coefficients (lift, drag, and side force; pitching, yawing, and rolling moment) and mass properties (mass and moments of inertia about the three axes). The aerodynamic coefficients were generated with the computer programs of Refs. 2 and 3.

The 6-DOF trajectory simulations[4] were used to compute impact footprints of the individual debris types. A typical Eastern Test Range (ETR) trajectory was chosen as the base case (Case 1, Table 1). State vectors at an altitude of 225,000 ft were used to initialize the 6-DOF trajectory simulation. In addition, three sets of randomly selected ET tumble rates (Table 2) were used for initial body rates. These different tumble rates were used with many combinations of angle of attack, angle of sideslip, and roll angle to obtain impact footprints of the individual debris types. From these footprints, mean and standard deviation range values were determined.

The 3-DOF simulations[5] were then used to obtain impact range values for a parametric variation of ballistic coefficient and lift-drag ration. From these 3-DOF range calculations

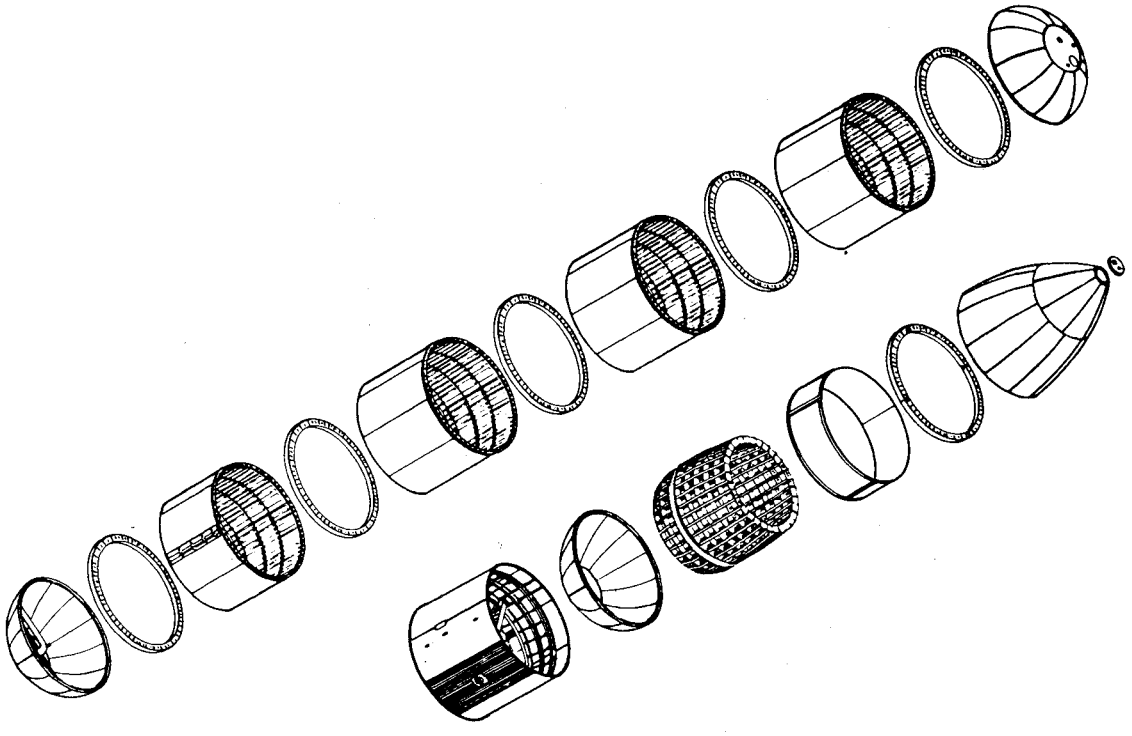

Fig. 1 External tank (exploded view).

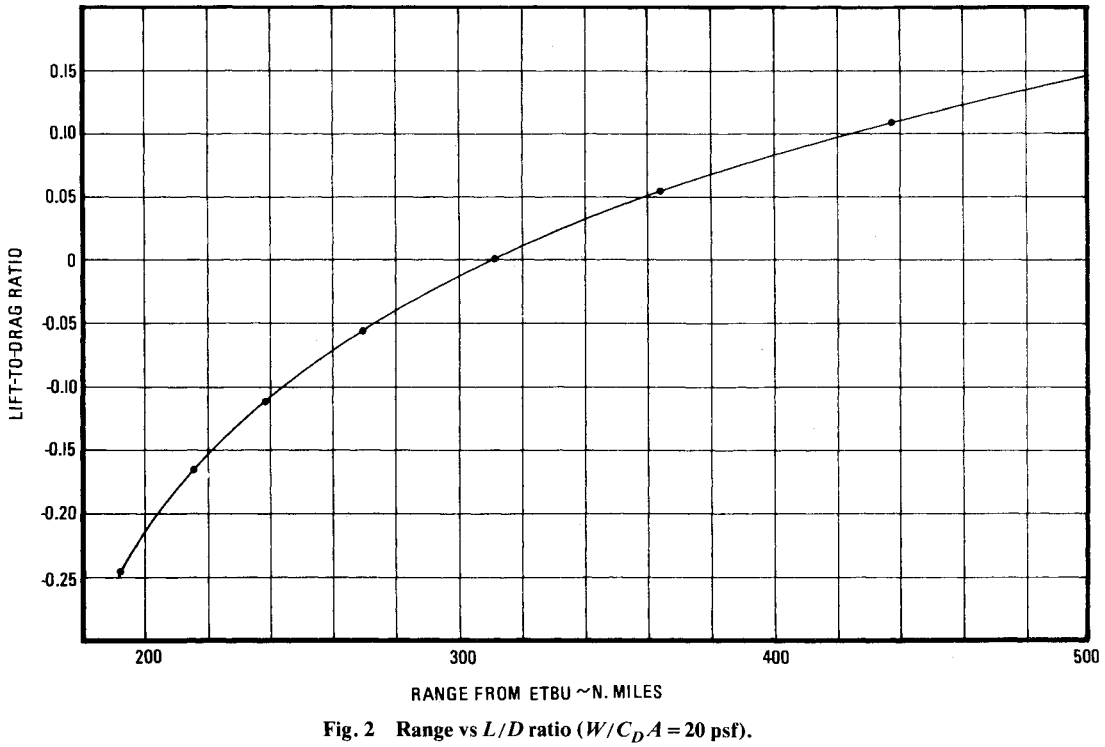

Fig. 2 Range vs L/D ratio ($W/C_DA = 20$ psf).

range vs L/D curves were generated for six W/C_DA values (Fig. 2 presents these data for $W/C_DA = 20$ psf). These data were then displayed on a single Range Increment Chart as illustrated in Fig. 3).

Two trajectories, in addition to the base case, were selected to test the hypothesis that the effective values of W/C_DA and L/D are independent of entry trajectory. Parameters for Case 2, with a Western Test Range (WTR) launch site, and Case 3, with an ETR launch site, are presented in Table 1.

For each of the previously defined debris types, two standard deviation range values (plus and minus) were marked on the Range Increment Chart. (For the example shown on Fig. 3, these range values were 348 and 282 n.mi.) The effective W/C_DA value was defined (assumption 4) as that which made the plus and minus L/D ratio values equal. In the example, the effective value of W/C_DA was found to be equal to 20 psf and the effective value of L/D was ± 0.040. The mean range had a 0.005 value for L/D.

The final effective values of W/C_DA and L/D were selected from results for the three trajectories to be most conservative. That is, the smallest W/C_DA values were selected for the shorter range debris types, the largest W/C_DA values were

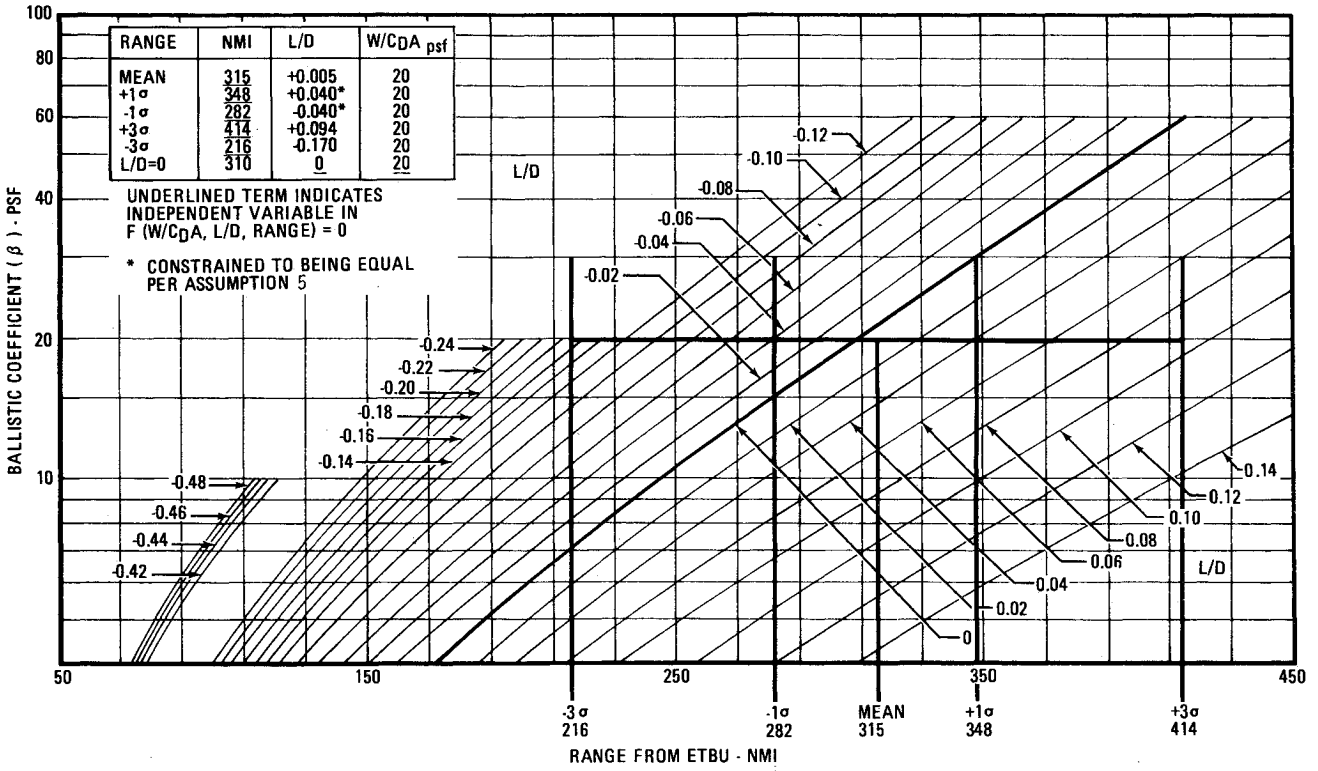

Fig. 3 Range increment chart.

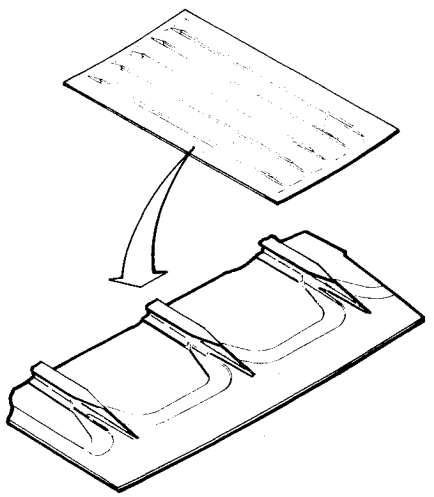

Fig. 4 Skin.

Table 1 Initialization parameters

Launch Site	Case 1 ETR (Base case)	Case 2 WTR	Case 3 ETR
Altitude, ft	225,045	200,393	199,924
Relative velocity, ft/s	23,393	20,496	22,963
Relative flight path angle, deg	−1.11	−2.94	−1.55
Initial dynamic pressure, psf	56	109	139

Table 2 Tumble rates for simulations

	Set 1	Set 2	Set 3
Pitch rate, deg/s	1.8	−0.9	−4.5
Yaw rate, deg/s	3.0	−3.9	−2.1
Roll rate, deg/s	−2.1	−2.7	−6.5

selected for the longer range debris types, and the largest L/D values were selected for all debris types.

Debris Types

Several individual studies were conducted on various types of ET debris to gain a better understanding of their behavior. These will be described with the results of each debris type.

Skin

The ET skin debris (Fig. 4) was the debris most extensively studied, since there was a concern that the skin debris pieces might skip, resulting in extremely long ranges. The skin can be classed into four basic configurations.

Skin-1: two-axis (X and Y) symmetry that has 0 distance between the center of gravity (c.g.) and the aerodynamic moment reference point (MRP).

Skin-2: Y-axis symmetry that has a lateral offset between the c.g. and MRP.

Skin-3: X-axis symmetry that has a longitudinal offset between the c.g. and MRP.

Skin-4: no symmetry, which has both lateral and longitudinal offsets between the c.g. and MRP. The skin size selected for this study was 12 ft long with an arc length of 3½ ft. Large 20 ft × 10 ft panels were also analyzed. Reference 1 presents a general description of all the debris types.

The skin-1 configuration had the largest range dispersion of any of the debris types analyzed and documented in this paper. This "typical" skin tended to tumble rather than trim like the skin-3 or "cone/spiral" like skin-2 and skin-4.

The ET disintegration analyses imply that the skin panels will tend to be 20 ft long and 10-20 ft wide. These large skin panels behave in a manner similar to the small "typical" skin panel. Both ends have thick skin for welding to ring frames.

Skin-1 produced the shortest impact range of all debris types. Effective values of W/C_DA and L/D for the three trajectories are presented in Table 3. To be conservative, the ET debris catalog will list the effective 3-DOF aerodynamic parameters for skin debris as: $W/C_DA = 5.1$ psf and

Table 3 3-DOF debris aerodynamic characteristics

	Case 1		Case 2		Case 3	
	W/C_DA, psf	$\sigma L/D$	W/C_DA,psf	$\sigma L/D$	W/C_DA, psf	$\sigma L/D$
Skin 1 (typical)	5.3	0.052	5.1	0.055	5.5	0.062
Skin 2[a]	9	0.065				
Skin 3[a]	13	0.092				
Skin 4[a]	5.5	0.060				
Ring frame	17.5	0.046	17	0.042		
Heavy pipe	34	0.018	35	0.018	35	0.018
Light pipe	18	0.020	18	0.019		
Intertank with domes	12.5	0.012	12.5	0.016		
Aft support structure	49	0.010	48	0.012	48	0.010

[a] Survival analyses indicate that these debris types would melt before impact.

Table 4 Ring frame results

Statistical results		Special simulations				
	Range, n.mi	Orientations	Initial conditions[a] α, deg	β, deg	Rates	Range, n.mi.
$+3\text{-}\sigma$	402					
$+1\text{-}\sigma$[b]	336	Edge facing into airstream	90	0	0	340.1
			0	90	0	339.2
Mean	303					
$L/D=0$	297		0	0	1000 deg/s	297.5
$-1\text{-}\sigma$[b]	270	Flat side facing into airstream	0	0	0	264.1
			0	0	"1"	264.0
			0	0	"2"	264.2
			0	0	"3"	266.5
$-3\text{-}\sigma$	209					

[a] α is the angle of attack; β is the angle of sideslip.
[b] Implies effective W/C_DA of 17.5 psf.

Table 5 Ring frame theoretical comparison (all $L/D=0$)

	Theoretical		6-DOF simulations	
	W/C_DA, psf	Range, n.mi.	W/C_DA, psf	Range, n.mi.
Average C_D ($L/D=0$)[a]	10.6	267	17.5	297.5[b]
Flat side forward	6.85	213	...	264
Edge forward	26.6	336	...	339

[a] Initial tumble rate = 1000 deg/s.
[b] $L/D=0$ for $W/C_DA=17.5$.

$L/D=0.0\pm0.062$. Survival analyses of the four skin types showed that most of the skin-1 type (including all that impacted outside the 1-σ standard deviation range) would melt and that all of the skin-2, -3, and -4 types would melt.

Ring Frames

The ring frame (Fig. 5) analyses provided orderly results. The ET has three sets of ring frames (Fig. 1) that may be included in the ET debris footprint. These include: 1) between the LO_2 tank ogive and barrel section, 2) between the LH_2 tank barrel sections 2 and 3, and 3) between the LH_2 tank barrels 3 and 4. The analysis implied an effective W/C_DA of 17.5 psf. The L/D ratio associated with the range data is 0.0 ± 0.040, with the mean having a 0.007 L/D ratio. The theoretical W/C_DA, based on a calculated average C_D, is 10.6 psf. The range associated with this W/C_DA is 267 n.mi., which is very near the 6-DOF $-1\text{-}\sigma$ range. A special ring frame trajectory simulation which had an initial 1000 deg/s tumble rate (and hence probably a 0 L/D ratio) landed within 0.5 n. mi., of the 0 L/D position for a 17.5 psf W/C_DA.

The theoretical W/C_DA for the ring facing forward (flat side facing into wind force) is 6.85 psf. This W/C_DA implies a 0 L/D range of 213 n.mi., just 9 n.mi from the $-3\text{-}\sigma$ range of 202 n.mi. This condition was subsequently simulated with 0 rates and the three mentioned rates of Table 2. All four of the trajectories had impact points near the $-1\text{-}\sigma$ range and landed within 2.74 mi. of each other.

Two edge-facing-forward trajectories were simulated. One had the flat side aligned perpendicular to the Earth's surface (angle of attack = 90 deg, angle of sideslip = 0 deg), while the other was aligned horizontal (angle of attack = 0 deg, angle of slideslip = 90 deg). Both of these simulations impacted near the $+1\text{-}\sigma$ range position and were within 0.4 n.mi of each other. They also landed within 4 n.mi. of the theoretical edge wide impact point based on a W/C_DA of 26.6 psf. The ring frame results (see Tables 4 and 5) summarize the aforementioned data and illustrate that ballistic coefficients derived directly from 6-DOF aerodynamic data are limited.

The three ring frames that could exist after ET disintegration will tumble in an orderly fashion and land near the middle of the complete ET debris footprint.

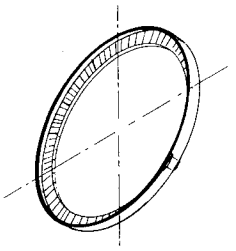

Fig. 5 Ring frame.

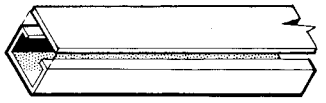

Fig. 6 Pipe tubing.

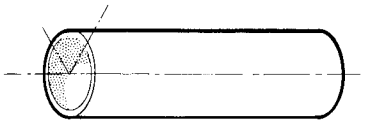

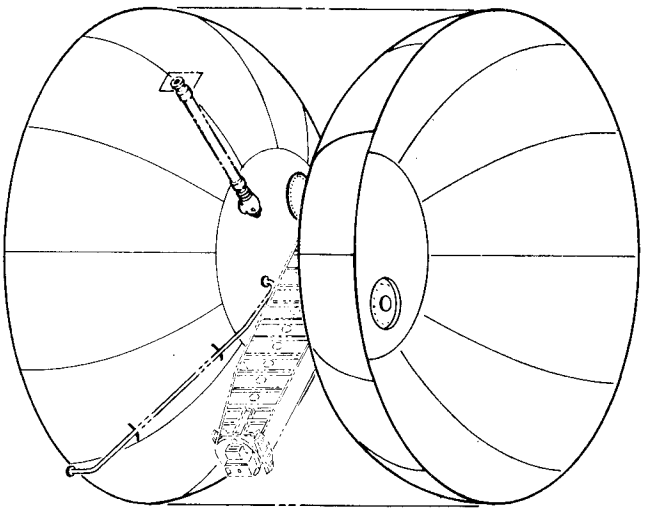

Fig. 7 Intertank with domes.

Pipe, Tubing, and Conduit

The pipe (Fig. 6) simulations show very orderly impact ranges for the three initial tumble rates analyzed. The three mean values were within 0.5 n.mi. of the total mean and the three standard deviation values were within 1.1 n.mi. of the total standard deviations. Pipes were simulated at two weights. The C_D values backed out of the W/C_DA values were very close to 3.02 for the "heavy" pipe vs 3.18 for the "light" pipe.

The pipe analysis confirmed the results of the ring frame analysis; i.e., ballistic coefficients based on the average drag coefficient do not always give desirable answers. For both pipe weights analyzed, 0 L/D trajectories (initial tumble ratio of 1000 deg/s) had actual range values almost equal to the theoretical W/C_DA (based on a calculated average C_D) with a 0 L/D ratio. However, with both pipe weights, these impact ranges were near the -3-σ range values determined from the 6-DOF trajectory simulations which used the low rates defined in Table 2. The case 1 trajectory data is summarized in Tables 6 and 7.

The "heavy" pipe effective W/C_DA and L/D characteristics derived for the case 1 trajectory showed good agreement with both case 2 and case 3 sets of 6-DOF trajectory simulations. The "light" pipe had essentially identical results for both the case 1 and case 2 analyses.

The W/C_DA values of 34 and 18 psf (heavy and light pipe/tubing) imply that this debris landed in the middle of the ET debris footprint. Survival analyses (Ref. 6) indicate that all of the tubing and conduits will melt, as well as the small diameter pipe. Large diameter aluminum pipe will have a small percentage survive to impact. The steel bellows in the feedline will survive and land in the far end of the footprint.

Intertank with Domes

The intertank with domes (Fig. 7) debris represents the mass between the LO_2 tank and the LH_2 tank. Most of the skin panels on the top and bottom of the intertank will probably have melted at ET disintegration. Those areas remaining will consist of: 1) the heavy side thrust panels used for transferring the SRB loads into the tank; 2) the SRB cross beam, which absorbs the moments from the SRB's; 3) four light and one heavy intermediate ring frames used for stiffening; and 4) the two domes from the propellant tanks.

Both the case 1 trajectory analysis and the case 2 trajectory analysis show this debris type having an effective W/C_DA of 12.5 psf. The corresponding L/D ratios associated with the standard deviation range value are 0.012 and 0.016 for case 1 and case 2 analyses, respectively. The larger value was used for the debris catalog valve.

The theoretical W/C_DA, based on the average C_D of this debris, is 10.7 psf. The range associated with the 10.7 psf and 0 L/D ratio is the same as the -2-σ range value derived from the 6-DOF trajectories.

Aft Support Structure

The aft support structure (Fig. 8), designed for transferring both the Shuttle Orbiter and SRB loads into the aft structure of the ET is built around the massive aft ring frame at station 2058. The Orbiter/ET attachment hardware includes the external structure, vertical struts, cross beam, diagonal strut,

Table 6 Case 1 trajectory 6-DOF pipe results

Pipe	Standard deviation range, n.mi.		Effective W/C_DA, psf	Effective L/D (1-σ)	3 Standard deviation range, n.mi.	
Heavy	351	379	34	±0.018	323	407
Light	290	322	18	±0.020	258	354

Table 7 Case 1 trajectory theoretical pipe results

Pipe	$W/C_D/A$, psf	Theoretical range, n.mi.	Range at 1000 deg/s tumble trajectories, n.mi.	Statistically derived 3-σ range, n.mi.
Heavy	24	329	326.4	323
Light	11.6	259	259.25	258

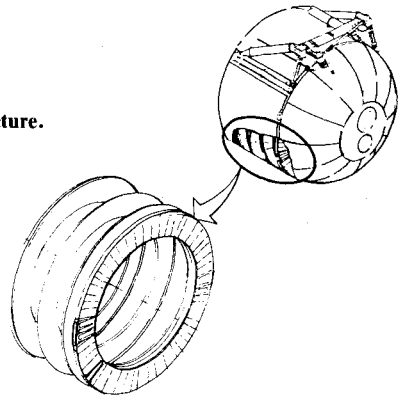

Fig. 8 Aft support structure.

thrust struts, and the longerons that transmit loads into the LH_2 tank, as well as the heavy ring at the forward end of the longerons (station 1971) and three stabilizing internal ring frames. The ET/SRB attach hardware includes four titanium attach forgings that are bolted at the station 2058 ring frame.

It is assumed that most of the LH_2 tank skin between the ring frames at stations 1871 and 2058 will have melted at ET disintegration. A small part of the aft LH_2 tank dome, which is attached to the 2058 ring frame, is included in this debris type.

The impact data from the 6-DOF trajectories are very compact, implying a very low L/D ratio. The extreme range of the debris type, the longest of any debris types defined from ET disintegration, implies a large W/C_DA value. This debris type exhibited consistent results for all three 6-DOF trajectory analyses as noted in Table 3.

The aft support debris has a very hot entry trajectory after ET disintegration (initially defined state vectors) since it enters above Mach 15 at 150,000 ft, and at Mach 4.5 at 100,000 ft. While the survival to impact of the complete debris type as defined is questionable, the effective ballistic coefficients of the members that do survive (pipe and ring frames) imply that the complete debris type would impact further down range than any of the parts (pipe and ring frames).

Results

The results of the study, the effective ballistic coefficients and lift-to-drag ratios, are presented in Table 3. The skin debris type has the smallest effective ballistic coefficient (W/C_DA of 5.1 psf) and thus forms the short end of the ET debris footprint. The aft support structure has the largest effective ballistic coefficient and, for most impact footprints, has the fartheset impact point. Table 8 presents the 3-σ results.

The effective ballistic coefficients with corresponding lift-to-drag ratios showed good agreement for all debris types examined between the case 1 and case 2 trajectory analyses. A third case was simulated for the typical skin, pipe, and aft support structure. These latter trajectory impact range data show good agreement, for these three debris types, with results for cases 1 and 2. Thus the hypothesis that the coefficients are independent of trajectory was confirmed. It should be noted in Table 3 that some debris types melt before impact and thus should not be considered as impact debris.

Table 8 Results for debris catalog

	W/C_DA, psf	L/D ratio[a] $-3\text{-}\sigma$	$+3\text{-}\sigma$
Skin	5.1	−0.465	0.130
Ring frame	17.5	−0.216	0.102
Light pipe	18	−0.070	0.054
Heavy pipe	34	−0.070	0.054
Intertank with domes	12.5	−0.054	0.043
Aft support structure	45	−0.039	0.033

[a] Effective—derived from $+3\sigma$ and $-3\text{-}\sigma$ range values.

Conclusions

A method has been developed for determining the effective aerodynamic characteristics for use in a 3-DOF (point mass) entry trajectory computer program. Development and application of this method has implied the following conclusions.

1) The methodology, as defined in this paper, is a valid means of determining effective 3-DOF aerodynamic characteristics (the point mass W/C_DA and L/D ratio) from 6-DOF entry trajectory analysis.

2) The previously used theoretical method (based on average 6-DOF drag coefficients) may be limited when analyzing debris from an External Tank entry trajectory. Significant differences between the theoretical W/C_DA values and the effective W/C_DA values were found with three of the four debris types examined.

3) The L/D ratio values of from -0.2 to $+0.2$ used in previous ET footprint determinations have been conservatively large.

4) The typical skin debris panels define the short end of the ET debris footprint.

5) The heavy aft ring frame attach support structure debris type defines the long end of the ET debris footprint.

Acknowledgments

The work was accomplished under NASA Contract NAS8-30300, dated May 17, 1973. John T. Stevens and Charles Crane of MSFC were contract monitors for the Marshall Space Flight Center. Robert B. Goss of MSFC provided assistance in the selecting of debris types for analysis. Donald Michna of the Martin Marietta Corporation determined the 6-DOF aerodynamic coefficients for the various debris types.

References

[1] Bonson, S.P., "Aerodynamic Characteristics for Selected ET Debris," Martin Marietta Corp., MMC-ET-SE05-63, Oct. 1975.

[2] Francisco, J., "A Computer Program to Calculate Static and Dynamic Force and Moment Coefficients on Complex Bodies," Martin Marietta Report D-73-48609-001, Dec. 1973.

[3] Gentry, A.E., "Hypersonic Arbitrary—Body Aerodynamic Computer Program (Mark III Version)," Douglas Report DAC 61552, April 1968.

[4] Stevenson, R., et al., "Equations and Logic for the UD214 Trajectory Simulation Program," Martin Marietta Corp., MMC, TM0472/10-70-07, Dec. 1970.

[5] Cornick, D.E., et al., "Capabilities and Applications of the Program to Optimize Simulated Trajectories (POST)," Martin Marietta Corp., NASA CR-2770, Feb. 1977.

[6] Sullivan, W.D., "User's Manual for the Lockheed Automated Parts Survival (LAPS) Computer Program," Lockheed, TM54/20-250, LMSC/HREC D 162140, May 1970.